

### 3.4 ESTIMATING SOIL LOSS

Soil loss estimates included in this report are based solely on June 2003 soil quality indicators and October 2002 remotely sensed data; estimates reflect soil loss risk only during the short, wet season of 2002/2003 (i.e., the rains succeeding the October harvest). Numerical estimates, therefore, are at best only an indicator of the relative magnitude of soil loss likely to have occurred over that period of time and, accordingly, are reported (in section 4.4)—and should only be interpreted—*qualitatively*. In the future, better approximations of soil loss could certainly be made if soil samples were collected *in situ* with remotely sensed data on, perhaps, a monthly basis. This would necessitate a cumulative application of—but not an inherent change to—the methodology described below.

Soil loss estimates were generated for each pixel (15 x 15 m<sup>2</sup> resolution) in the village by importing ASTER DN<sub>s</sub> (VNIR, MIR, slope, and altitude) for all village pixels with valid DEM data and slopes less than 25° (169,001 of 187,707 total) into Excel<sup>TM</sup> spreadsheets. Estimates were derived based on the factors included in the Universal Soil Loss Equation (USLE), which is shown in its original form below.

$$A = R \cdot K \cdot (L \cdot S) \cdot C \cdot P \quad (3.8)$$

Where,

**A** = average annual soil loss [10<sup>3</sup> kg/(ha·yr)]

**R** = erosivity (N/h)

**K** = erodibility [t·h/(ha·N)]

**L** = slope length factor (dimensionless)

**S** = slope steepness factor (dimensionless)

**C** = land cover factor (dimensionless)

**P** = soil protection factor (dimensionless)

DEM altitude data are used to calculate the R-factor and slope data for the L · S factors. The K-factor relies on averages of soil quality indicators (clay and C<sub>org</sub>) for

each land use/soil type, whereas the C and P factors are based on the October ASTER image's VNIR and DEM DN values. For all factors, higher values cause a direct increase in annual soil loss. The following sections describe how all factors are calculated to produce soil loss estimates based on their application to the village of Kambi ya Simba.

### ***Erosivity (R)***

This factor represents the kinetic energy of falling raindrops (splash) as well as that from running water (wash). It is expressed in the units N/h, where N is equal to  $\text{kJ/m}^2 \cdot \text{mm}$  (the kinetic energy of one millimeter of erosive rainfall over a square meter) and h is equal to one hour. Rainfall energy in the USLE is calculated as (3.9).

$$E = (11.89 + 8.73 \cdot \log I) \cdot n \cdot 10^{-3} \quad \text{for } I < 76.2 \text{ mm/h} \quad (3.9)$$

Where,

$$\begin{aligned} E &= \text{Energy (kJ/m}^2\text{)} \\ I &= \text{intensity (mm/h)} \\ n &= \text{total rainfall (mm)} \end{aligned}$$

The R-value is calculated as the summation of all *erosive* storm events' E-values for an entire year multiplied by the average maximum 30-minute intensity. As detailed storm data are unavailable for Kambi ya Simba, R-values were calculated for a given elevation's average annual rainfall (20+ years of data) from the linear equation shown in Figure 3.4.1, and based on a constant average intensity of 6.7 mm/h and a constant average maximum 30-minute intensity of 25 mm/h. The average maximum intensity of 25 mm/h is recommended by Hudson (1971) for East Africa, as it is the threshold value at which rainfall becomes erosive on clayey soils. While rainfall intensities greater than or equal to 25 mm/h only occur in 6% of East Africa's total storm events,

these events account for over 70% of the total rainfall per year (Edwards et al., 1979). Annual rainfall values used in calculations are thus reduced to 70% of their original values. The average intensity of 6.7 mm/h is an estimate derived from the distribution of intensities during storm events that reach the maximum intensity of 25 mm/h (Figure 3.4.2). A 1% increase in kinetic energy of raindrops that occurs per 100 m increase in elevation (Van Dijk et al., 2002) is also accounted for. By combining equation (3.9) with these considerations and the linear equation shown in Figure 3.4.1, equation (3.10) shows the entire calculation for the R-factor. Figure 3.4.3 shows how R-factor values vary by altitude (due to changes in annual rainfall).

$$R = (11.89 + 8.73 \cdot \log I) \cdot X \cdot (a \cdot h - b) \cdot I_{30} \cdot 1.01^{h/100} \cdot 10^{-3} \quad (3.10)$$

Where,

I = intensity (mm/h) [I = 6.7 mm/h, E. Africa]

$I_{30}$  = avg. max. 30-minute intensity (mm/h) [ $I_{30}$  = 25 mm/h, E. Africa]

X = % of annual rainfall considered erosive (X = 0.70, E. Africa)

a = slope of rainfall/altitude equation (a = 0.9732, K/S)

b = y-intercept of rainfall/altitude equation (b = 740.61mm, K/S)

h = elevation (masl)

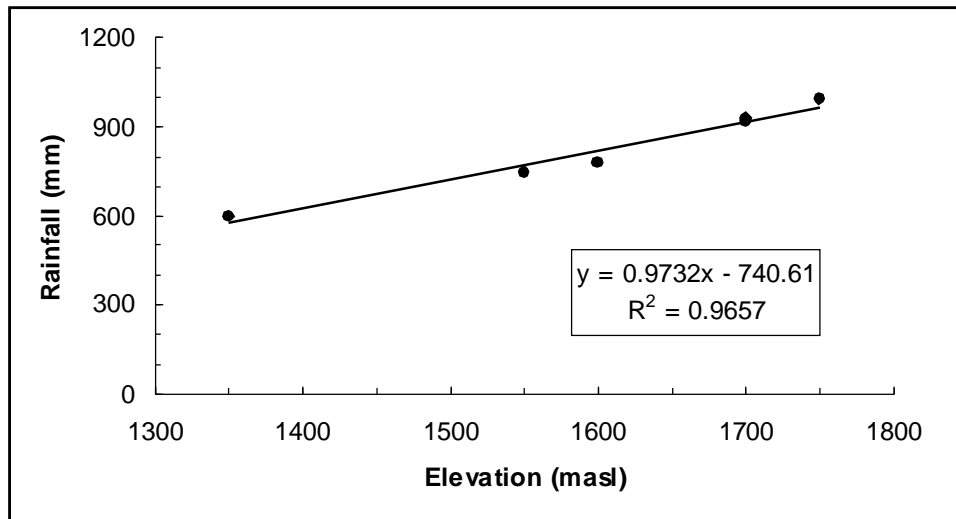
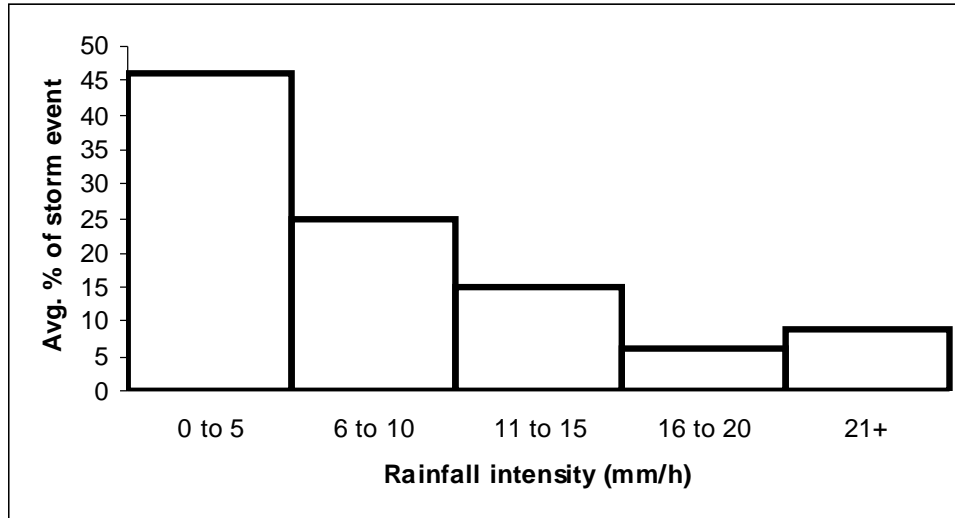
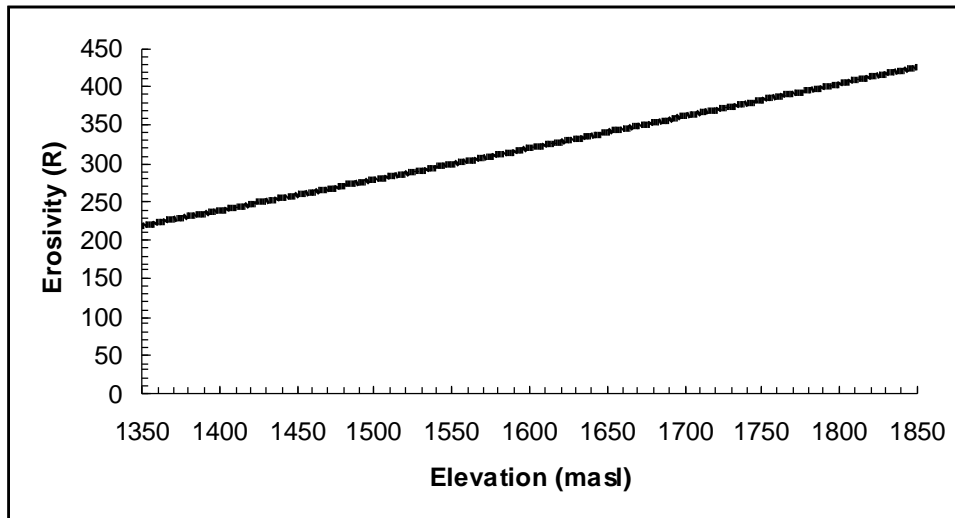


Figure 3.4.1 Altitudinal rainfall gradient for Kambi ya Simba (cf. data in Magoggo, 1997)



**Figure 3.4.2** Average distribution of rainfall intensities during storm events for East Africa (adapted from Edwards et al., 1983)



**Figure 3.4.3** Erosivity (R-factor) by elevation (as a product of average annual rainfall) in Kambi ya Simba village

### ***Erodibility (K)***

The K-factor is expressed in the units  $(10^3 \text{ kg/ha}) / [(kJ/m^2) \cdot (mm/h)]$  or  $(10^3 \text{ kg}\cdot\text{h}) / (\text{ha}\cdot\text{N})$ . Erodibility of topsoil is controlled by its organic matter content, aggregation status, permeability, and clay content. It appears in the USLE as (3.11).

$$K = 2.77 \cdot 10^{-6} \cdot M^{1.14} \cdot (12 - OM) + 0.043 \cdot (A - 2) + 0.033 \cdot (4 - D) \quad (3.11)$$

Where,

OM = organic matter content

A = mean aggregate grain size class

{1: < 1 mm, 2: 1-2 mm, 3: 2-10 mm, 4: > 10 mm }

D = permeability (rate of infiltration) class

{6: very slow, 5: slow, 4: slow to moderate

3: moderate, 2: moderate to rapid, 1: rapid }

M = (100 - % clay) · (% silt + % very fine sand)

All of the soils in Kambi ya Simba are dominantly clay/silt, therefore, all soil types were assumed to have mean aggregate grains sizes less than 1 mm (class 1) and slow rates of infiltration (class 5), as recommended by Wenner (1981).

Several factors, however, complicate calculation of the M-values in the equation. First, soil samples were sieved prior to grain size analysis to less than 2 mm, so the quantity of particles greater than 2 mm is unknown (although, based on observations, it would be negligible for most samples). Second, grain size analysis was only reported for bulk weight contents of clay/silt/sand and so actual grain size distributions within silt and sand particles are unknown. This is only problematic for sand, as sand grain sizes range from 0.05 to 2.0 mm but the ‘very fine sand’ grain sizes needed for ‘M’ only range from 0.05 to 0.125 mm. Third, bulk silt and sand contents are only known for the 10 soil samples selected for laboratory analysis, as grain sizes larger than clay have not been calibrated to soil spectra. Thus, due to these limitations, M-values had to be extrapolated from clay content for all soil samples based on the logarithmic relationship between maximum grain size and the cumulative bulk weight percentage for each grain size class in the 10 known samples (Figure 3.4.4). Based on the regression equation in Figure 3.4.4, grains less than 0.125 mm diameter should account for 68.3% of bulk sample weight and 44.6% of all

grains in the silt to very fine sand range. This latter factor is incorporated into the M-value equation included in equation (3.11) as (3.12).

$$\begin{aligned}
 M &= 0.446 \cdot (\% \text{ silt} + \% \text{ very fine sand}) \cdot (100 - \% \text{ clay}) \\
 &= 0.446 \cdot (100 - \% \text{ clay})^2
 \end{aligned}
 \tag{3.12}$$

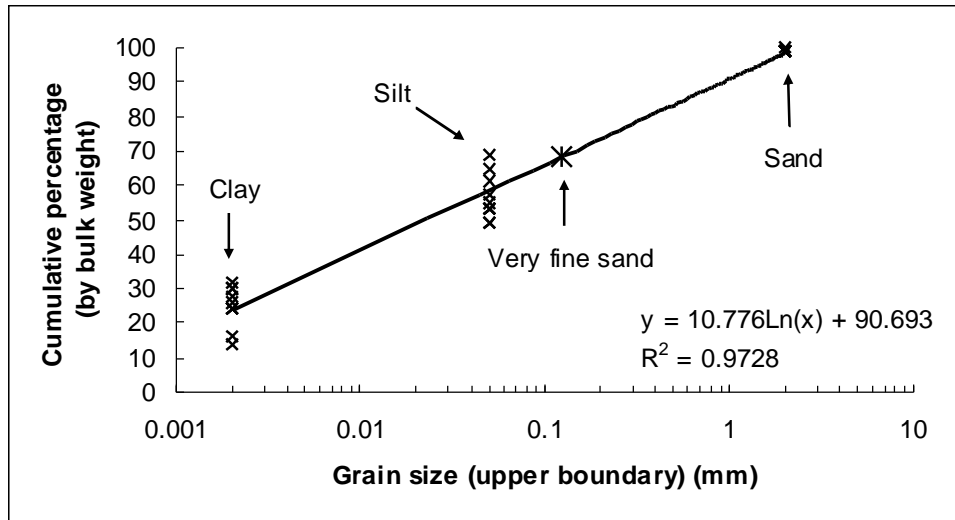


**Figure 3.4.4** Logarithmic plot of grain size diameter by cumulative bulk weight percentage for the 10 soil samples selected for laboratory analysis

One of the original goals of this project was to determine each ASTER pixel's clay and organic matter content (for input into the K-factor) by calibrating soil quality indicators derived from soil spectra to the ASTER images. This was attempted by matching the quality indicators of all 100 soil samples to VNIR-MIR ASTER DN's for both October and June images. PLS regression was performed using all 18 DN's (i.e., 3 VNIR + 6 MIR for each image) and ASTER DEM altitude; however, all  $r^2$  values were less than 0.4 and adjusted  $r^2$  values less than 0.2, so the calibration was not considered successful.

In lieu of calibration, values for OM and M were assigned to each pixel in the village based on the averages for each land use type within each soil type (these

values appear as appendix). For example, a pixel remotely defined as ‘dense bush/graze’ and of soil type RL2 would be assigned OM and M values based on the average DRS-predicted values of  $C_{org}$  and clay content for ‘bush’ soil samples in RL2. Sampled fields were not separated into the remotely defined categories of ‘residues’ and ‘bare’, as residue management practices visible in June 2003 are not necessarily indicative of practices employed in October 2002. Table 3.4.1 shows how the nomenclature used for on-site land use classification was transferred to the nomenclature of remotely based land use classification.

In some instances, a soil sample was not collected for each land use type within each soil type and in these instances OM and M values are shared by different land use types within a soil type (also indicated in appendix). Where applicable, sharing only occurs between the two bush/graze land use types (i.e., ‘dense’ and ‘sparse’ share values).

**Table 3.4.1** On-site land use categories and their respective remotely defined categories

On-site category	Site description	Remotely defined category
Bush	Canopy > 25%, surface cover > 75%	Bush/graze – dense
Graze	Dominantly grassland with tree/shrub canopy < 25%	Bush/graze – sparse
Field	Crops present or fallow	Field
Eroded <sup>2</sup>	Rills or gullies with variable cover	Variable

A factor of 1.724 was multiplied to  $C_{org}$  values for conversion to soil organic matter content, as recommended by Jackson (1958). Organic matter contents greater than 7.0 are outside the predictive range of the USLE and should not be used in the equation (all Kambi ya Simba sample averages had OMC values below 7.0), (Jones et al., 1996). Figure 3.4.5 illustrates the relationships between clay/OMC and the K-factor.

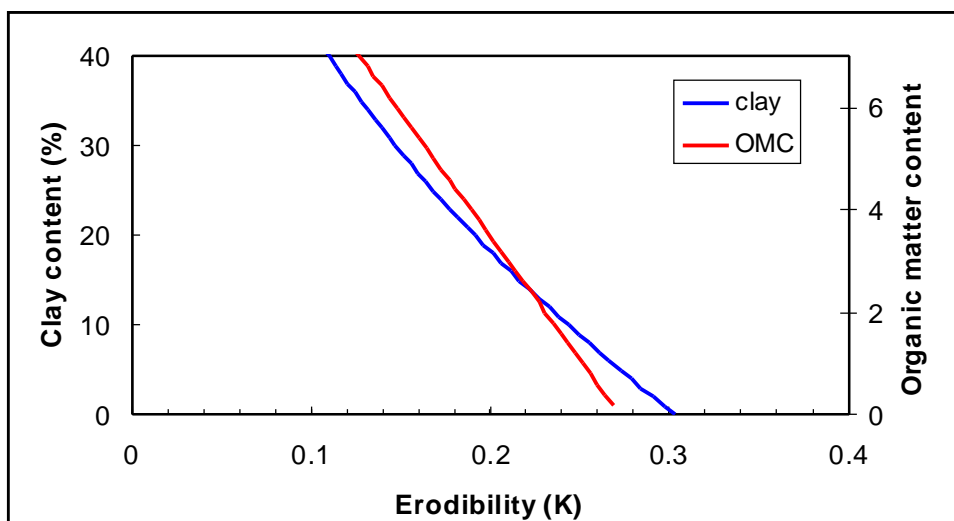


**Figure 3.4.5** Erodibility (K-factor) by clay content and OMC for Kambi ya Simba  
 \*clay curve based on constant OMC = 5; OMC curve based on constant clay content = 25%.

### *Slope length (L)*

The slope length factor quantifies the length ( $\ell$ ) in the direction of main water flow (runoff) as its deviation from the USLE standard plot ( $\ell = 22.1$  m). It is calculated in the USLE as (3.13).

$$L = (\ell/22.1)^m \quad (3.13)$$

Where,

$$m = \text{slope (\% class value)} \\
\{0.15: \leq 0.5\%, 0.2: 0.6-1.0\%, 0.3: 1.1-3.4\%, \\
0.4: 3.5-4.9\%, 0.5: \geq 5.0\%\} \\
\ell = \text{length}$$

To solve for  $\ell$ , the following equation is used:

$$\ell = 15 / \cos(s) \quad s = \text{slope (}^\circ\text{)} \quad (3.14)$$

This latter equation (3.14) relies on the assumption that the average pixel has a width of 15 m (the spectral resolution of the adjusted DEM) and hence its slope length is equal to the hypotenuse of the right triangle (where  $\theta = s$ ). When substituted back into the original equation, L can be solved for solely in terms of s and m:

$$L = (0.6787 / \cos(s))^m \quad (3.15)$$

### ***Slope steepness (S)***

The slope steepness factor is based on a plot's deviation from the USLE standard of 9%. It is calculated as:

$$S = 65.41 \cdot \sin^2 s + 4.56 \cdot \sin s + 0.065 \quad s = \text{slope } (^\circ) \quad (3.16)$$

Figure 3.4.4 shows the relationship between slope and the  $L \cdot S$  factor; slope of  $\sim 5.85^\circ$  is the threshold at which the  $L \cdot S$  factor begins to contribute to increased soil loss (i.e.,  $L \cdot S > 1.0$ ).

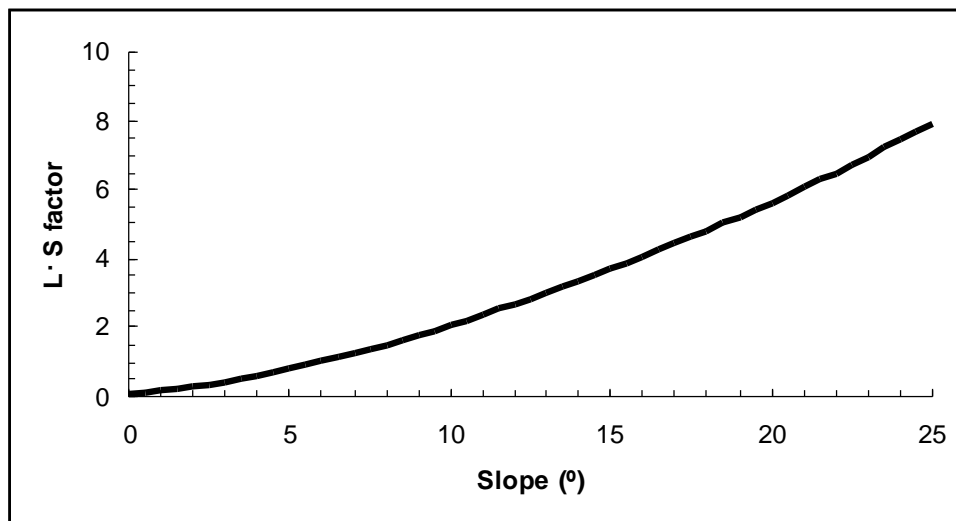


**Figure 3.4.6** Slope-derived factors in the USLE

### ***Cropping (C) and protection (P)***

C and P factors are based on the degree of protection afforded by vegetative cover against erosive forces. Because it is not possible to tell whether fields are properly tilled or employ vegetated contour ridges, the P-factor is combined with the C-factor to derive qualitative soil loss estimates. In the USLE, C and P factors are derived from look-up tables; however, a modified version of these factors is calculated in the

SLEMSA (Soil Loss Estimation Model for Southern Africa), which is based solely on rainfall energy interception (I), and can be applied to land use types other than fields (the USLE was designed mainly for agricultural applications). This equation appears from Elwell (1978) as (3.17).

$$\begin{aligned} C &= e^{-0.06 \cdot I}, \text{ for } I < 50\% \\ C &= (2.3 - 0.01 \cdot I)/30, \text{ for } I \geq 50\% \end{aligned} \quad (3.17)$$

For the purposes of this study, it is assumed that rainfall energy interception is equal to canopy cover, as most direct contact with the canopy will reduce the (splash) force of raindrops such that they are no longer erosive to soil. To make a more thorough estimate of rainfall energy interception, however, factors such as raindrop and leaf angle (this study assumes all raindrop-leaf collisions are perpendicular) and plant height would also need to be considered.

Canopy cover is equivalent to the Fraction of Photosynthetically Active Radiation ( $f_{PAR}$ ), which has already been presented as equation (3.3). As SLA-NDVI generates the same range of values as NDVI (-1.00 to 1.00) and was found to be a more sensitive index to the Kambi ya Simba data set (Table 4.2.3), the SLA-NDVI value for each pixel was used in lieu of NDVI.  $f_{PAR}$  values from equation (3.3) were then substituted for rainfall energy interception in equation (3.17) to solve for the C-factor for each pixel. Again, only the DNs from the October image were used in these calculations, as the majority of rainfall events that could be considered erosive occur before June (i.e., before crops reach maturity at the beginning of the dry season). Figure 3.4.7 shows the curvilinear relationship of SLA-NDVI values to C-factor values, as calculated by equations (3.17) and (3.3).

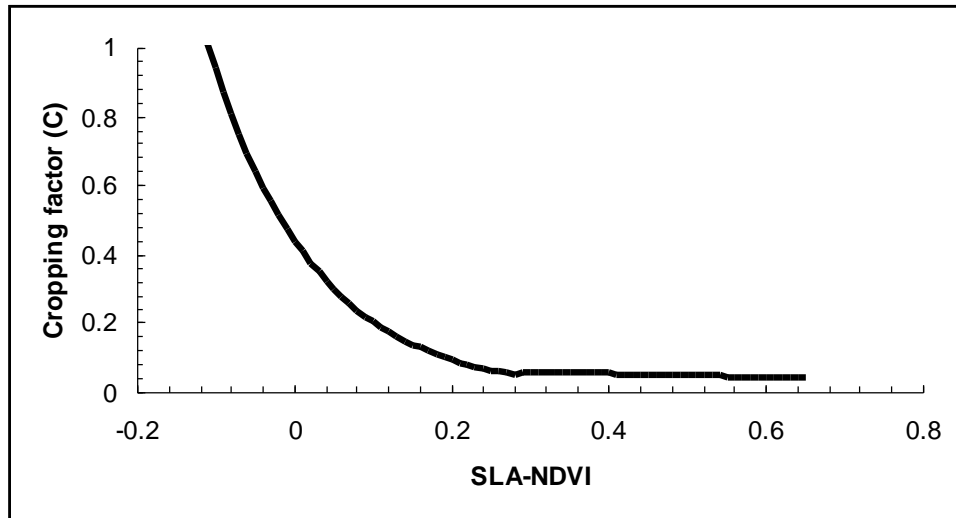


Figure 3.4.7 Cropping factor values generated by October SLA-NDVI values

### *Applying the soil loss equation*

Table 3.4.2 illustrates the weight of each variable used in the soil loss equation, calculated as the percent deviation from an arbitrary, “standard” bare field. From this table, it is clear that the slope variable holds the greatest weight in the equation, followed by SLA-NDVI (i.e., canopy cover) and then clay/organic matter content. However, as the individual factors used in the soil loss equation do not exhibit linear relationships with their variables (with the exception of elevation and the R-factor), the relative weight of each variable can vary considerably throughout its range of values (e.g., in Table 3.4.2, a reduction to -0.1 from the “standard” SLA-NDVI value of 0.0 causes an 11.4% increase in soil loss, while an increase from 0.0 to 0.1 only causes a 5.3% decrease in soil loss despite the fact that absolute SLA-NDVI changes are equivalent).

**Table 3.4.2** Weight of variables used in generating soil loss estimates

Elevation (m)	SLA-NDVI	% clay	OMC	Slope (°)	A [ $10^3$ kg/(ha·yr)]	Deviation
1500	0.0	25.0	5.0	1.0	3.03	std.
std.	-0.1	std.	std.	std.	6.49	+11.4%
std.	0.1	std.	std.	std.	1.42	-5.3%
std.	0.2	std.	std.	std.	0.66	-7.8%
std.	0.5	std.	std.	std.	0.35	-8.8%
1650	std.	std.	std.	std.	3.70	+2.2%
1350	std.	std.	std.	std.	2.38	-2.1%
std.	std.	15.0	std.	std.	3.90	+2.9%
std.	std.	35.0	std.	std.	2.30	-2.4%
std.	std.	std.	3	std.	3.78	+2.5%
std.	std.	std.	7	std.	2.29	-2.5%
std.	std.	std.	std.	2.0	5.60	+8.5%
std.	std.	std.	std.	4.0	12.5	+31.1%
std.	std.	std.	std.	8.0	33.7	+101.2%
std.	std.	std.	std.	16.0	109.5	+351.0%

After estimating soil loss (and estimating soil loss without the slope factors) for each pixel in the village with valid DEM data and slope less than 25°, all village pixels were sorted into 15 groups based on their relative soil loss “ranking” (1 being the lowest amount of soil loss and 15 being the highest). For each ranking group, pixels were imported back into ENVI as ROIs and then color coded in Adobe Photoshop to produce soil loss maps.

Numerical values for soil loss were tested for significant, Pearson product-moment correlations against June (pre-harvest) SLA-NDVI and MSI indices. Since DN values from the June image were not included in the soil loss equation, these tests were performed to assess the degree to which soil loss estimates could offer improved prediction of vegetation density over October (post-harvest) SLA-NDVI and MSI values. As October DNs are included in the soil loss equation (via SLA-NDVI into the C-factor), a significant correlation between soil loss estimates and June vegetation would not be meaningful if there is an implicit, equal or greater correlation between October and June vegetation (i.e., the soil loss estimates have a strong correlation to

the June image only because there is already a strong correlation between the DNs in the two images). On the other hand, if soil loss correlations are stronger than implicit DN correlations, this suggests that improved prediction of pre-harvest vegetation health/density necessitates the inclusion of factors exogenous to post-harvest vegetation (i.e., elevation/rainfall energy, clay/OMC, and slope). In this project, the latter outcome is more desirable, as it adds validity to the methodology used to generate the soil loss estimates.